

STOCHASTIC LOEWNER EVOLUTION

Linking universality, criticality and conformal invariance in complex systems

Hans C. Fogedby

Aarhus University, Aarhus, Denmark
and
Niels Bohr Institute, Copenhagen, Denmark

ARTICLE OUTLINE

- I. Introduction
 - A. General Remarks
 - B. Scaling Ideas
 - C. Scaling in Equilibrium
 - D. Stochastic Loewner Evolution
 - E. Outline
- II. Scaling
 - A. Random Walk
 - B. Percolation
 - C. Ising Model
 - D. Critical curves - Exploration
 - E. Distributions - Markov properties - Measures
- III. Conformal Invariance
 - A. Conformal Maps
 - B. Measures - Conformal Invariance
- IV. Loewner Evolution
 - A. Growing Stick
 - B. Loewner Equation
 - C. Exact Solutions
- V. Stochastic Loewner Evolution
 - A. Schramm's Theorem
 - B. SLE Properties
 - C. Curves and Hulls - Bessel Process
 - D. Fractal Dimension
- VI. Results and Discussion
 - A. Phase transitions - Locality - Restriction - Duality
 - B. Loop Erased Random Walk
 - C. Self Avoiding Random Walk
 - D. Percolation
 - E. Ising model - $O(n)$ Models
 - F. SLE - Conformal Field Theory
 - G. SLE - 2D Turbulence
 - H. SLE - 2D Spin glass
 - I. Further remarks
- VII. Future Directions
- VIII. Bibliography

I. INTRODUCTION

Stochastic Loewner evolution also called Schramm Loewner evolution (abbreviated, SLE) is a rigorous tool in mathematics and statistical physics for generating and studying scale invariant or fractal random curves in two dimensions (2D). The method is based on the older deterministic Loewner evolution introduced by Karl Löwner [76], who demonstrated that an arbitrary curve not crossing itself can be generated by a real function by means of a conformal transformation. A real function defined in one spatial dimension (1D) thus encodes a curve in 2D, in itself an intriguing result. In 2000 Oded Schramm [82] extended this method and demonstrated that driving the Loewner evolution by a 1D Brownian motion, the curves in the complex plane become scale invariant; the fractal dimension turns out to be determined by the strength of the Brownian motion.

The one-parameter family of scale invariant curves generated by SLE is conjectured and has in some cases been proven to represent the continuum or scaling limit of a variety of interfaces and cluster boundaries in lattice models in statistical physics, ranging from self-avoiding random walks to percolation cluster boundaries, and Ising domain walls.

SLE operates in the 2D continuum where it generates extended scale invariant objects. SLE delimits scaling universality classes by a single parameter κ , the strength of the 1D Brownian drive, yielding the fractal dimension D of the scale invariant shapes according to the relation $D = 1 + \kappa/8$. Moreover, SLE provides the geometrical aspects of conformal field theory (CFT). The central charge c , delimiting scaling universality classes in CFT, is thus related to κ by means of the expression $c = (3\kappa - 8)(6 - \kappa)/2\kappa$.

Stochastic Loewner evolution derives its' importance from the fact that it addresses the issue of extended random fractal shapes in 2D by direct analysis in the continuum. It thus supplements and extends earlier lattice results and also allows for the determination of new scaling exponents. From the point of view of conformal field theory based on the concept of a local field, operator expansions, and correlations, the geometrical approach afforded by SLE, directly addressing conformally invariant random shapes in the continuum, represents a novel point of view of maybe far reaching consequences; so far only explored in two dimensions.

The field of SLE has mainly been driven by mathematicians presenting their results in long and difficult papers. There are, however, presently several excellent reviews of SLE both addressing the theoretical physics community [5,6,12,13,21,57] and the mathematical community [24,35], see also a complete biography up to 2003 [57]. The purpose of this article is to present a heuristic and simple discussion of some of the key aspects of SLE, for details and topics left out we refer the reader to the reviews mentioned above. However, in order provide the necessary background and set the stage for SLE we begin with some general remarks on scaling in statistical physics.

A. General Remarks

In statistical physics we study macroscopic systems composed of many interacting components. In the limit of many degrees of freedom the macroscopic behavior roughly falls in two categories. In the most common case the macroscopic behavior is deterministic and governed by phenomenological theories like for example thermodynamics and hydrodynamics operating entirely on a macroscopic level. This behavior is basically a result of the law of large numbers, permitting an effective coarse graining and yielding for example a macroscopic density or velocity field [14]. In the other case, the macroscopic behavior is dominated by fluctuations and shows a random behavior [14,31]. Typical cases are random walk and equilibrium systems tuned to the critical point of a second order phase transition. Other random cases are for example self-organized critical systems purported to model earth quake dynamics, flicker noise and turbulence in fluids [4,20].

The distinction between the deterministic and random cases of macroscopic behavior is illustrated by the simple example of a biased random walk described by the Langevin equation $dx(t)/dt = v + \xi(t)$, $\langle \xi(t)\xi(0) \rangle \propto \delta(t)$. Here $x(t)$ is a macroscopic variable sampling the statistically independent microscopic steps $\xi(t)$; the velocity v is an imposed drift or bias. Averaging over the steps we obtain for the deviation of x , $R = [\langle x^2 \rangle]^{1/2} = [(vt)^2 + t]^{1/2}$. For large t the deviation $R \sim \langle x \rangle = vt$ and the mean value or deterministic part dominates the behavior, the fluctuational or random part $R \sim t^{1/2}$ being subdominant. Fine tuning the random walk to vanishing bias $v = 0$ we have $\langle x \rangle = 0$ and $R \sim t^{1/2}$, i.e., the random fluctuations control the phenomenon.

The study of complexity encompasses a broader field than statistical physics and is concerned with the emergence of universal properties on a mesoscopic or macroscopic scale in large interacting systems. For example particle systems, networks in biology and sociology, cellular automata, etc. The class of complex systems generally falls in the category of random systems. The emergent properties are a result of many interacting agents or degrees of freedom and can in general not be directly inferred from the microscopic details. A major issue is thus the understanding of generic emerging properties of complex systems [22,28,34]. Here, however, the methods of statistical physics is an indispensable tool in the study of complexity.

The evolution of statistical physics, a branch of theoretical physics, has occurred in steps and is driven both by the introduction of new concepts and the concurrent development of new mathematical methods and techniques. A well-known case is the long standing problem of second order phase transitions or critical phenomena which gave way to a deeper understanding in the sixties and seventies and spun off the renormalization group techniques for the determination of critical exponents and universality classes [8,11,26,32,36].

B. Scaling Ideas

This brings us to the fundamental scaling ideas and techniques developed particularly in the context of critical phenomena in equilibrium systems and which now

pervade a good part of theoretical physics and, moreover, play an important role in the analysis of complex systems in physical sciences [8,11,14]. Scaling is synonymous with no scale in the sense that a system exhibiting scale invariance is characterized by the absence of any particular scale or unit. Scaling occurs both in the space and/or time behavior and is typically characterized by power law dependencies controlled by scaling exponents.

A classical case is random walk discussed above, characterized by the Langevin equation $dx/dt = \xi(t)$, $\langle \xi \xi \rangle \sim \delta(t)$ [31]. Here the mean square displacement scales like $\langle x^2 \rangle(t) \sim t^{2H}$, where H is the Hurst scaling exponent; for random walk $H = 1/2$ [16,27]. Correspondingly, the power spectrum $P(\omega) = |x_\omega|^2$, $x_\omega = \int dt x(t) \exp(i\omega t)$, scales like $P(\omega) \sim \omega^{-1-2H}$, i.e., $P(\omega) \sim \omega^{-2}$ for random walk; we note that the underlying reason for the universal scaling behavior of random walk is the central limit theorem [18,31].

C. Scaling in Equilibrium

Scaling ideas and associated techniques first came to the forefront in statistical physics in the context of second order phase transitions or critical phenomena [8,11,14,26]. More specifically, consider the usual Ising model defined on a lattice with a local spin degrees of freedom, $\sigma_i = \pm 1$ at site i , subject to a short range interaction J favoring spin alignment. The Ising Hamiltonian has the form $H = -J \sum_{\langle ij \rangle} \sigma_i \sigma_j$, where $\langle ij \rangle$ indicates nearest neighbor sites. The thermodynamic phases are characterized by the order parameter $m = \langle \sigma_i \rangle$. Above one dimension the Ising model exhibits a second order phase transition at a finite critical temperature T_c . Above T_c the model is in a disordered paramagnetic state with $m = 0$ and only microscopic domain of ordered spins. Below T_c the model favors a ferromagnetic state with long range order and macroscopic domains of ordered spins, corresponding to $m \neq 0$; at $T = 0$ the model assumes the ferromagnetic ground state configuration with totally aligned spins. Regarding the spatial organization, the size of the domains of ordered spins is characterized by the correlation length $\xi(T)$. As we approach the critical point at T_c the order parameter vanishes $m \propto |T - T_c|^\beta$ with critical exponent β , but more significantly, the correlation length $\xi(T)$ diverges like $\xi(T) \sim |T - T_c|^{-\nu}$ with scaling exponent ν . This indicates that the system is scale invariant at T_c . Regarding the domains of ordered spins, the system is spatially self-similar on scales from the microscopic lattice distance to the system size; the system size diverging in the thermodynamic limit. The scaling behavior at the critical point T_c is an emergent property in the sense that the scaling exponents β and ν do not depend on microscopic details like the type of lattice, strength of interaction, etc., but only on the dimension of the system and the symmetry of the order parameter [30].

The diverging correlation length at the critical point is the central observation which in the 60-ties and 70-ties gave rise to a detailed understanding of critical phenomena, beginning with the coarse graining block scheme proposed by Kadanoff [58] and culminating with the development and application of field theoretical renormalization group techniques by Wilson and others [8,11,14,26,30,36].

For a diverging correlation length much larger than the lattice distance the local spin σ_i can be replaced by a coarse-grained local field $\phi(r)$ and the Ising Hamiltonian H by the Ginzburg-Landau functional $F = \int d^d r [(\nabla\phi)^2 + R\phi^2 + U\phi^4]$, where the 'mass' term $R \sim |T - T_c|$. Consequently, the universality class of Ising-type models is described by a scalar field theory. The renormalization group techniques basically quantify the Kadanoff block construction in momentum space and extract scaling properties in an expansion about the upper critical dimension $d = 4$. To leading order in $4 - d$ one obtains $\beta = 1/2 - (4 - d)/6$ and $\nu = 1/2 + (4 - d)/12$ (Wilson 1974). Alternatively, keeping the correlation length ξ fixed and letting the lattice distance approach zero, we obtain at T_c the so-called scaling limit or continuum limit of the Ising model. The Ising spin σ_i becomes a local field $\phi(r)$ and the weight of a configuration is determined by $\exp(-F)$. Note that in order to implement the scaling limit we must be at T_c . The two scenarios of a growing correlation length for fixed lattice distance implementing the Kadanoff construction and a fixed correlation length for a vanishing lattice distance yielding a continuum field theory are related by an overall scale transformation [36].

It is generally assumed that the global or nonlocal scale invariance at the critical point in the continuum limit can be extended to a local scale invariance including translation and rotation, that is an angle-preserving conformal transformation. This follows heuristically from an a local implementation of the Kadanoff coarse-graining block construction and applies to lattice models with short range interactions and discrete translational and rotational invariance [9,11]. The resulting continuum theories then fall in the category of conformal field theories (CFT).

In 2D the group of conformal transformations is particularly rich since it corresponds to the class of analytical functions $w = f(z)$ mapping the complex plane z to the complex plane w . The infinite group structure imposes sufficient constraints on the structure of conformal field theories in 2D that the scaling form of correlations, e.g., $\langle\phi\phi\rangle(r)$, and in particular the critical exponents can be determined explicitly [10,11]. One finds $\beta = 1/8$ and $\nu = 1$ for the order parameter and correlation length exponents, respectively, in accordance with lattice theory results (Baxter 1982). Here we also mention the Coulomb gas method for the determination of critical exponents [29].

It is a common feature of both renormalization group calculations based on an expansion about a critical dimension and conformal field theory in 2D that the local field $\phi(r)$ and its correlations are the basic building blocks and that the critical properties are encoded in their scaling form, yielding critical exponents, scaling laws, scaling functions, etc. Notwithstanding the fact that the seminal Kadanoff construction [58] was based on a geometrical picture corresponding to coarse-graining the degrees of freedom over larger and larger scales, keeping track of ordered domains on all scales, the actual geometry of critical phenomena such as the scaling properties of critical clusters was not well-understood and seemed inaccessible in the continuum limit within the context of local field theories. Whereas it is not difficult to generate critical domain walls, interfaces, and clusters for lattice models with appropriate boundary conditions by means of standard Monte Carlo simulation techniques, the continuum or scaling limit of critical shapes appeared until recently, with a few exceptions, beyond present techniques.

D. Stochastic Loewner Evolution

Here stochastic Loewner evolution (SLE) represents a new insight in 2D critical phenomena with respect to a deeper understanding of scale invariant curves, clusters, and shapes. Also, there appears to be deep connections between SLE and conformal field theory.

SLE is an ingenious way of generating critical curves and shapes in the 2D continuum using conformal transformations. Let us mention a characteristic example. Consider an Ising model on a lattice in a chosen domain. Imposing spin up on a continuous part of the domain boundary and spin down on the remaining part of the boundary, it follows that a specific domain wall or interface will connect the two points on the boundary where a bond is broken. At low temperature the bond energies dominate and the free energy is lowest for a straight domain wall with few kinks. As we approach the critical point entropy or fluctuations come strongly into play and the domain wall meanders balancing energy and entropy. At the critical point the system becomes scale invariant with a diverging correlation length and likewise the domain wall becomes scale invariant, i.e., it has kinks on all scales larger than the lattice distance. In the continuum limit the Ising domain wall becomes a random fractal curve with a particular fractal dimension. Here SLE provides a direct analytical method in the continuum to generate such a random curve and, moreover, provides the fractal dimension in terms of the strength of the 1D random walk driving the SLE evolution.

E. Outline

The outline of the present particle is as follows. In Section III on scaling we introduce some of the basic models and concepts necessary for a discussion of SLE: A) Random walk, B) Percolation, C) Ising model, D) Critical curves and exploration, and E) Distributions, Markov properties, and measures. In Section IV we turn to the essential ingredient in SLE, namely, conformal invariance: A) Conformal maps and B) Measures and conformal invariance. Section V is devoted to deterministic or classical Loewner evolution: A) Growing stick, B) Loewner equation and C) Exact solutions. In Section VI, constituting the core part of this article, we discuss stochastic Loewner evolution: A) Schramm's theorem, B) SLE properties, C) Curves, hulls, and the Bessel process and D) Fractal dimension. Section VII is devoted to results and discussions: A) Phase transitions, locality, restriction, and duality, B) Loop erased random walk, C) Self-avoiding random walk D) Percolation, E) Ising model and $O(n)$ models, F) SLE and conformal field theory, G) Application to 2D turbulence, H) Application to 2D spin glass and I) Further remarks. Finally, in Section VIII we discuss future directions of the field. Section IX contains a bibliography including books, general reviews, and more technical papers.

II. SCALING

Stochastic Loewner evolution, has been applied to a host of lattice models proved or conjectured to possess scaling limits. However, for the present purpose we will focus on three lattice models: Random walk, Percolation, and the Ising model.

A. Random Walk

Random walk is a simple and much studied random process [3,16,31]. Consider an unbiased random walk in the plane composed of N steps, where the i -th step, $\vec{\eta}_i$, is random, isotropic and uncorrelated, i.e., $\langle \vec{\eta}_i \rangle = 0$ and $\langle \eta_i^\alpha \eta_j^\beta \rangle \propto \delta_{\alpha\beta} \delta_{ij}$. For the end-to-end distance we have $\vec{x} = \sum_{i=1}^N \vec{\eta}_i$ and for the size $R = [\langle \vec{x}^2 \rangle]^{1/2} \sim N^{1/2}$. Assuming one step pr unit time, $N \propto t$, we obtain $R \sim t^{1/2}$, characteristic of diffusive motion. Introducing the fractal dimension D by the usual box counting procedure [16,27]

$$N(R) \sim R^D, \quad (2.1)$$

where N is the number of boxes and R the size of the object, and covering the random walk we readily infer $D = 2$, i.e., the self-crossing random walk is plane-filling modulo the lattice distance. Introducing the scaling exponent ν according to $R \sim N^\nu$ we have for random walk $\nu = 1/2$; note that $D = 1/\nu$.

The scaling limit of unbiased random walk is Brownian motion (BM) [3] and is obtained by scaling the step size η down and the number of steps N up in such a manner that the size $R \sim N^{1/2}\eta$ stays constant. The resulting BM path is a continuous non-differentiable random curve with fractal dimension $D = 2$. The BM path is plane-filling and recurrent in 2D, i.e., it returns to a given point with probability one. Focussing on one of the independent cartesian components 1D BM, B_t , is also described by the Langevin equation

$$\frac{dB_t}{dt} = \eta_t, \quad \langle \eta_t \eta_s \rangle = \delta(t - s), \quad (2.2)$$

where η_t is uncorrelated Gaussian white noise with a flat power spectrum. Integrating Eq. (2.2) B_t samples the step η_t and we find, assuming $B_0 = 0$, $B_t = \int_0^t \eta_{t'} dt'$ from which we directly infer the fundamental properties of BM, namely, independence and stationarity,

$$B_{T+\Delta T} - B_T \approx B_{\Delta T}, \quad (\text{stationarity}) \quad (2.3)$$

$$B_{\Delta T}, B_{\Delta T'} \text{ indep. for } \Delta T \neq \Delta T', \quad (\text{independence}) \quad (2.4)$$

where \approx indicates identical distributions. Moreover, the correlations are given by

$$\langle |B_t - B_s|^2 \rangle = |t - s|. \quad (2.5)$$

and B_t is distributed according to the normal (Gaussian) distribution $P(B, t) = (2\pi t)^{-1/2} \exp(-B^2/2t)$.

Whereas 1D BM drives SLE, 2D BM is not itself generated by SLE since the path is self-crossing on all scales; by construction SLE is limited to the generation of

non-crossing random curves. However, variations of BM have played an important role in the development of SLE. We mention here the scaling limit of loop erased random walk (LERW) and self-avoiding random walk (SAW), to be discussed later.

B. Percolation

The phenomenon of percolation is relevant in the context of clustering, diffusion, fractals, phase transitions and disordered systems. As a result, percolation theory provides a theoretical and statistical background to many physical and natural sciences [33].

Percolation is the simplest lattice model exhibiting a geometrical phase transition. The site percolation model is constructed by occupying sites on a lattice with a given common probability p . Let an occupied site be denoted 'plus' and an 'empty' site denoted 'minus'. For p close to zero the sites are mainly unoccupied and the lattice is 'minus'. For p close to one the sites are predominantly occupied and the lattice is 'plus'. At a critical concentration p_c , the percolation threshold, an infinite cluster of 'plus' sites embedded in the 'minus' background extends across the lattice. In the scaling limit of vanishing lattice distance the critical cluster has a fractal boundary which can be accessed by SLE. Whereas the scaling properties of critical percolation clusters define a universality class and is independent of the lattice structure, the critical concentration p_c in general depends on the lattice. For site percolation on a triangular lattice the percolation threshold is known to be $p_c = 1/2$.

In Fig.1 we depict a realization of site percolation on a triangular lattice in the upper half plane at the percolation threshold $p_c = 1/2$. The occupied sites are denoted 'plus', the empty sites 'minus'. By imposing appropriate boundary conditions we induce a meandering domain wall across the system from A to B. In the scaling limit the domain wall becomes a fractal non-crossing critical curve.

C. Ising Model

The Ising model is probably the simplest interacting many particle system in statistical physics [8,14,32]. The model has its origin in magnetism but has become of paradigmatic importance in the context of phase transitions. The model is defined on a lattice where each lattice site i is occupied by a single degree of freedom, a spin variable σ_i , assuming two values, $\sigma_i = \pm 1$, i.e., spin up or spin down. In the ferromagnetic case considered here the spins interact via a short range exchange interaction J favoring parallel spin alignment. The model is described by the Ising Hamiltonian

$$H = -J \sum_{\langle ij \rangle} \sigma_i \sigma_j, \quad (2.6)$$

where $\langle ij \rangle$ indicates nearest neighbor spin sites i and j . The statistical weight or probability of a specific spin configuration $\{\sigma_i\}$ is determined by the Boltzmann

factor

$$P(\{\sigma_i\}) = \exp[-H/kT]/Z, \quad (2.7)$$

where T is the temperature and k Boltzmann's constant. The partition function Z has the form

$$Z = \sum_{\{\sigma_i\}} \exp(-H/kT), \quad (2.8)$$

yielding the thermodynamic free energy F according to $F = -kT \log Z$. The entropy is given by $S = -dF/dT$ and the energy follows from $F = E - TS$. The magnetization or order parameter and correlations are given by

$$m = \sum_{\{\sigma_i\}} \sigma_i P(\{\sigma_i\}) \quad \text{and} \quad \langle \sigma_i \sigma_j \rangle = \sum_{\{\sigma_i\}} \sigma_i \sigma_j P(\{\sigma_i\}), \quad (2.9)$$

respectively.

The Ising model possesses a phase transition at a critical temperature T_c from a disordered paramagnetic phase above T_c with vanishing order parameter $m = 0$ to a ferromagnetic ordered phase below T_c with non-vanishing order parameter $m \neq 0$. At the critical temperature T_c the order parameter vanishes like $m \sim |T - T_c|^\beta$ with critical exponent β . The correlation function $\langle \sigma_i \sigma_j \rangle$ monitoring the spatial organization of ordered domains behaves like

$$\langle \sigma_i \sigma_j \rangle \sim \frac{\exp[-|i - j|/\xi]}{|i - j|^\eta}, \quad (2.10)$$

where η is a critical exponent and the correlation length ξ scales like $\xi \sim |T - T_c|^{-\nu}$ with critical exponent ν . At the critical point the correlation length ξ diverges and the Ising model becomes scale invariant with an algebraically decaying correlation function $\langle \sigma_i \sigma_j \rangle \sim |i - j|^{-\eta}$. Assigning 'plus' to spin up and 'minus' to spin down, Fig.1 also illustrates a typical configuration of the 2D Ising model on a triangular lattice at the critical temperature, including an Ising domain wall from A to B.

D. Critical curves - Exploration

In the percolation case at the percolation threshold a critical curve is induced by fixing the boundary conditions. Occupying sites from A to B along the right hand side of the boundary and assigning empty sites along the left hand side of the boundary from A to B a critical curve will meander across the system from A to B . Imagining painting the two sides of the curve, one side is painted with occupied sites, the other side with empty sites. Typically the curve meanders on all scales but by construction does not cross itself. For later purposed the configuration is depicted in Fig. 1.

In order to make contact with SLE we observe that a critical interface in the percolation case also can be constructed by an exploration process. We initiate the curve at the boundary point A and toss a coin. In the case of 'head' the site or

hexagon in front is chosen to be occupied and the path bends left; in the event of 'tail' the hexagon in front is left unoccupied and the path bends right. In this manner a critical meandering non-crossing curve is generated terminating eventually at B . The percolation growth process is depicted in Fig. 2, where we for clarity only have indicated the sites involved in the growth process. We note that since there is no interaction between the sites the path depends entirely on the local properties.

In the case of the Ising model a critical interface or domain walls at the critical point is again fixed by assigning appropriate boundary conditions with spin up along the boundary from A to B and spin down from B to A . The critical curve can be constructed in two ways: Globally or by an exploration process. In the global case we generate a spin configuration by means of a Monte Carlo simulation, i.e., perform a biased importance sampling implementing the probability distribution in Eq. (2.7), and identify a critical interface. Alternatively, we can generate an interface by an exploration process like in the percolation case, occupying a site i according to the weight $(1/2)(1 + \langle \sigma_i \rangle)$, where $\langle \sigma_i \rangle$ is evaluated in the domain with the spins along the interface fixed, see again Fig. 2.

E. Distributions - Markov properties - Measures

In the case of random walk the number of walks of length L grows like μ^L , where μ is a lattice dependent number, i.e., at each step there are μ lattice-dependent choices for choosing a direction of the next step. Consequently, the weight or probability of a particular walk of length L is proportional to μ^{-L} ,

$$P(L) \sim \mu^{-L}, \quad (2.11)$$

and all walks of a given length have the same weight. We note here the important Markov property, characteristic of random walk, which can be formulated in the following manner. Assume that the first part γ' of the walk has taken place and thus conditions the remaining part γ of the walk. In a suggestive notation the conditional distribution is given by $P(\gamma|\gamma') = P(\gamma\gamma')/P(\gamma')$. The Markov property implies that the conditional probability is equal to the probability of the walk γ in a new domain where the first part of the walk γ' has been removed, i.e., the identity

$$P(\gamma|\gamma') = P'(\gamma), \quad (\text{Markov property}) \quad (2.12)$$

where the prime refers to the new domain. The Markov property is self-evident for random walk and follows directly from Eq. (2.11), i.e., $P(\gamma|\gamma') = P(\gamma\gamma')/P(\gamma') = \mu^{-(L+L')}/\mu^{-L'} = \mu^{-L} = P'(\gamma)$, where L and L' are the lengths of segments γ' and γ , respectively.

In the scaling limit the lattice distance goes to zero whereas the length of the walk diverges. Consequently, the distribution diverges and must be replaced by an appropriate probability measure [3,6,21]. However, in order to define the probability distribution or measure in the scaling limit we shall assume that the Markov property continues to hold and interpret the P in Eq. (2.12) as probability measures. The Markov property is essential in carrying over the lattice probability distributions in the scaling limit.

For the critical interfaces defined by an exploration processes in the case of site percolation, the Markov property follows by inspection since the propagation of the interface is entirely determined by the local process of occupying the next site with probability $1/2$. This locality property is specific for percolation which has a geometrical phase transition and does in the SLE context, to be discussed later, determine the scaling universality class.

In the case of an interface in the Ising model the Markov property also holds, but since the spins interact a little calculation is required [6]. Consider an interface γ defined by an exploration process. According to the rules of statistical mechanics the probability distribution for the interface γ is given by

$$P(\gamma) = \frac{Z(\gamma)}{Z}. \quad (2.13)$$

Here Z is the full partition function defined in Eq. (2.8) with appropriate boundary conditions imposed. $Z(\gamma)$ is the partial partition function with the spins associated with the interface γ fixed,

$$Z(\gamma) = \sum_{\{\sigma_i\}, \gamma} \exp[-H(\gamma)/kT]. \quad (2.14)$$

The Hamiltonian $H(\gamma)$ inferred from Eq. (2.6) is the energy of a spin configuration with the spins determining γ fixed; $\{\sigma_i\}, \gamma$ indicate the configurations to be summed over. Evidently, we have the identity $Z = \sum_{\gamma} Z(\gamma)$, i.e., $\sum_{\gamma} P(\gamma) = 1$.

Whereas in the random walk case we only considered an individual path and in the percolation case the interface only feels the nearby sites, an Ising interface is imbedded in the interacting spin systems and we have to define the Markov property more precisely with respect to a domain D . Consider an interface across the domain D from A to B and assume that the last part γ is conditioned on the determination of the first part γ' , i.e., given by the distribution $P_D(\gamma|\gamma')$. Next imagine that we cut the domain D along the interface γ' , i.e., break the interaction bonds between the spins determining γ' . The right and left face of γ' can then be considered part of the domain boundary and the Markov property states that the distribution of γ in the cut domain $D \setminus \gamma'$ (i.e., D minus γ') equals $P_D(\gamma|\gamma')$,

$$P_D(\gamma|\gamma') = P_{D \setminus \gamma'}(\gamma). \quad (\text{Markov property}) \quad (2.15)$$

In order to demonstrate Eq. (2.15) we use the definition in Eq. (2.13). The conditional probability $P_D(\gamma|\gamma') = P_D(\gamma\gamma')/P_D(\gamma') = (Z_D(\gamma\gamma')/Z_D)/(Z_D(\gamma')/Z_D) = Z_D(\gamma\gamma')/Z_D(\gamma')$. Correspondingly, the distribution in the cut domain $D \setminus \gamma'$ is $P_{D \setminus \gamma'}(\gamma) = Z_{D \setminus \gamma'}(\gamma)/Z_{D \setminus \gamma'}$. However, it follows from the structure of the partition function in Eqs. (2.6 - 2.8) that $Z_{D \setminus \gamma'} = \exp[E(\gamma')/kT]Z_D(\gamma')$ and $Z_{D \setminus \gamma'}(\gamma) = \exp[E(\gamma')/kT]Z_D(\gamma\gamma')$, where $E(\gamma')$ is the energy of the broken bonds. By insertion the interface Boltzmann factors cancel out and we obtain Eq. (2.15) expressing the Markov property.

III. CONFORMAL INVARIANCE

In the complex plane analysis implies geometry. The representation of a complex number $z = x + iy$ directly associates complex function theory with 2D geometrical

shapes. This connection is of importance in mathematical physics in for example 2D electrostatics and 2D hydrodynamics . In the context of SLE Riemann's mapping theorem plays an essential role [1].

A. Conformal Maps

Briefly, Riemann's mapping theorem [2] states that any simply connected domain, i.e., topologically deformable to a disk, in the complex plane z can be uniquely mapped to a unit disk $|w| < 1$ in the complex w plane by mean of a complex function $w = g(z)$. By combining complex functions we can map any simply connected domain to any other simply connected domain. For example, if $g_1(z)$ and $g_2(z)$ map domains D_1 and D_2 to the unit disk, respectively, then $g_2^{-1}(g_1(z))$ maps D_1 to D_2 ; here g_2^{-1} is the inverse function of g_2 , i.e., $g_2^{-1}(g_2(z)) = z$. As an example, the transformation $g(z) = i(1+z)/(1-z)$ maps the the unit disk centered at the origin to the upper half plane. Likewise, the Möbius transformation $g(z) = (az+b)/(cz+d)$ determined by four real parameters, $ad - bc > 0$, maps the upper half plane onto itself. Conformal transformations are angle-preserving and basically correspond to a combination of a local rotation, local translation, and local dilatation. In terms of an elastic medium picture conformal transformations are equivalent to deformations without shear (Landau 1959). Expressing $g(z)$ in terms of its real and imaginary parts, $g(z) = u(x, y) + iv(x, y)$, the Cauchy-Riemann equations $\partial u/\partial x = \partial v/\partial y$ and $\partial u/\partial y = -\partial v/\partial x$ hold implying that u and v are harmonic functions satisfying Laplace's equations $\nabla^2 u = 0$ and $\nabla^2 v = 0$, $\nabla^2 = \partial^2/\partial x^2 + \partial^2/\partial y^2$. In Fig. 3 we have depicted a conformal angle-preserving transformation effectuated by the complex function $g(z)$ from the complex z plane to the complex w plane.

B. Measures - Conformal Invariance

Whereas the Markov property discussed above holds for lattice curves even away from criticality, we here want to assume another property which only holds in the scaling limit at the critical point, namely conformal invariance. In the scaling limit we anticipate that the probability measure $P(\gamma)$ for an interface γ is invariant under a conformal transformation. More precisely, consider a lattice model, say the Ising or percolation model, and specify two domains D and D' on the lattice. Next, consider an interface, cluster boundary or domain wall γ from the boundary points A and B across the domain D . In terms of the partition functions the probability distribution for γ is given by Eq. (2.13). We now perform the scaling or continuum limit of the lattice model keeping the domains D and D' fixed. The continuous random interface approaches its scaling form and is characterized by the measure $P_D(\gamma)$. At the critical point we assume that the interface is scale invariant under the larger symmetry of conformal transformations. The next step is to consider a specific conformal transformation $g(z)$ which according to Riemann's theorem precisely maps domain D to domain D' , i.e., $D' = g(D)$ and the interface to $g(\gamma)$. The assumption of conformal invariance then states that the probability measure P

is invariant under this transformation expressing the scale invariance, i.e.,

$$P_D(\gamma) = P_{g(D)}(g(\gamma)). \quad (\text{Conformal property}) \quad (3.1)$$

Both the Markov property and the conformal property are sufficient in combination with Loewner evolution to determine the measures in the scaling limit.

IV. LOEWNER EVOLUTION

The original motivation of Loewner's work was to examine the so called Bieberbach conjecture which states that $|a_n| \leq n$ for the coefficients in the Taylor expansion $f(z) = \sum_{n=0} a_n z^n$. The conjecture was proposed in 1916 and finally proven in 1984 by de Branges [2,19,57]. For that purpose Loewner [76] considered growing parametrized conformal maps to a standard domain. In the present context Loewner's method allow us to access growing shapes in 2D in an indirect manner by means of a 'time dependent' conformal transformation $g_t(z)$.

A. Growing Stick

Before we address the derivation of the Loewner equation let us consider the specific conformal transformation

$$g_t(z) = \sqrt{z^2 + 4t}. \quad (4.1)$$

For $t = 0$ we have $g_0(z) = z$, i.e., the identity map. Likewise, for $z \rightarrow \infty$ we obtain

$$g_t(z) \sim z + \frac{2t}{z}, \quad (4.2)$$

showing that far away in the complex plane we again have the identity map. The coefficient in the next leading term, C_t/z , is called the capacity C_t ; here parametrized by the 'time variable', $t = C_t/2$. The map (4.1) has a branch point at $z = 2it^{1/2}$ and it follows by inspection that g_t maps the upper half plane minus a stick from the origin $\mathbf{0}$ to $2it^{1/2}$ back to the upper half plane. From the inverse map $f_t(w) = g_t^{-1}(w)$,

$$f_t(w) = \sqrt{w^2 - 4t}, \quad (4.3)$$

we infer that the right face of the stick is mapped to the real axis from 0 to $2t^{1/2}$, the tip to the origin, and the left face to the interval $-2t^{1/2}$ to 0. Under the map the growing stick thus becomes part of the boundary in the w plane. The growing stick is depicted in Fig. 4.

The stick shows up as an imaginary contribution along the interval $-2t^{1/2}$ to $2t^{1/2}$. More precisely, since $f_t(w)$ is analytic in the upper half plane, implementing the asymptotic behavior $f_t(w) \sim w$ for $w \rightarrow \infty$, and using Cauchy's theorem, we obtain the dispersion relation or spectral representation

$$f_t(w) = w - \int \frac{d\omega}{\pi} \frac{A_t(\omega)}{w - \omega}, \quad (4.4)$$

with spectral weight $A_t(\omega)$. In the case of the growing stick we find $A_t(\omega) = (4t - \omega^2)^{1/2}$ for $\omega^2 < 4t$ and otherwise $A_t(\omega) = 0$. Using $1/(\omega + i\epsilon) = \text{P } 1/\omega - i\pi\delta(\omega)$ (P denotes principal value) we also have $\text{Im}f_t(\omega) = A_t(\omega)$ and $\text{Re}f_t(\omega) = \omega - \text{P} \int (d\omega'/\pi) A_t(\omega')/(\omega - \omega')$. The time dependent spectral weight $A_t(\omega)$ thus characterizes the growing stick. With the chosen parametrization we also have the sum rule

$$\int \frac{d\omega}{\pi} A_t(\omega) = C_t = 2t. \quad (4.5)$$

Finally, we note that the map g_t satisfies the equation of motion

$$\frac{dg_t(z)}{dt} = \frac{2}{g_t(z)}, \quad (4.6)$$

i.e., solving Eq. (4.6) with the initial condition $g_0(z) = z$ and the boundary condition $g_t(z) \sim z$ for $z \rightarrow \infty$ we arrive at the map in Eq. (4.1).

B. Loewner Equation

The growing stick nicely illustrates the idea of accessing a growing shape indirectly by the application of Riemann's theorem mapping the domain adjacent to the shape to a standard reference domain, here the upper half plane. This so-called uniformizing map effectively absorbs the shape and encodes the information about the shape into the spectral weight $A_t(\omega)$ along the real axis.

Let us consider a general shape or hull \mathbf{K}_t in the upper half plane \mathbf{H} . Together with the real axis the shape form part of the boundary of the domain \mathbf{D} . In other words, the domain in question is the upper half plane \mathbf{H} with the shape \mathbf{K}_t subtracted, $\mathbf{D} = \mathbf{H} \setminus \mathbf{K}_t$. Applying Riemann's theorem we map the simply connected domain \mathbf{D} back to the upper half plane \mathbf{H} by means of the conformal transformation $g_t(z)$, i.e., g_t absorbs the shape \mathbf{K}_t . Imagine that the shape grows a little bit further from \mathbf{K}_t to $\mathbf{K}_{t+\delta t} = \mathbf{K}_t + \delta\mathbf{K}_t$, where \mathbf{K}_t is now part of $\mathbf{K}_{t+\delta t}$; $\delta\mathbf{K}_t$ is the shape increment. Correspondingly, the map $g_{t+\delta t}$ is designed to absorb $\mathbf{K}_{t+\delta t}$, i.e., $\mathbf{H} \setminus \mathbf{K}_{t+\delta t} \rightarrow \mathbf{H}$ by means of the map $g_{t+\delta t}$. We now carry out the elimination in two ways. Either we absorb \mathbf{K}_t by means of the map g_t and subsequently $\delta\mathbf{K}_t$ by means of the map δg_t or we absorb $\mathbf{K}_{t+\delta t}$ directly in one step by means of the map $g_{t+\delta t}$. Consequently, combining maps we have $g_{t+\delta t}(z) = \delta g_t(g_t(z))$ or $g_t(z) = \delta g_t^{-1}(g_{t+\delta t}(z))$. Since $\delta g_t^{-1}(w)$ is analytic in \mathbf{H} we obtain the spectral representation

$$\delta g_t^{-1}(w) = w - \int \frac{d\omega}{\pi} \frac{\delta A_t(\omega)}{w - \omega}, \quad (4.7)$$

with infinitesimal spectral weight δA_t , or inserting $w = g_{t+\delta t}(z)$

$$g_t(z) = g_{t+\delta t}(z) - \int \frac{d\omega}{\pi} \frac{\delta A_t(\omega)}{g_{t+\delta t}(z) - \omega}. \quad (4.8)$$

The last step is to set $\delta A_t(\omega) = \rho_t(\omega)\delta t$, yielding a differential equation for the evolution of the map g_t eliminating the shape \mathbf{K}_t ,

$$\frac{dg_t(z)}{dt} = \int \frac{d\omega}{\pi} \frac{\rho_t(\omega)}{g_t(z) - \omega}. \quad (4.9)$$

Specifying the weight or measure $\rho_t(\omega)$ along the real ω -axis this equation determines, through the uniformizing map g_t , how the shape \mathbf{K}_t grows. The spectral weight encodes the 2D shape into the real function $\rho_t(\omega)$. Note that since $\rho_t(\omega)$ is not specified and can depend nonlinearly on the map, Eq. (4.9) still represent a highly nonlinear problem. Invoking the asymptotic condition $g_t(z) \sim z + C_t/z$, where C_t is the time dependent capacity we infer $dC_t/dt = \int (d\omega/\pi) \rho_t(\omega)$ or since $\rho_t(\omega) = dA_t(\omega)/dt$ the sum rule in Eq. (4.5). The conformal mapping procedure is depicted in Fig. 5.

In the special case where the growth takes place at a point the equation simplifies considerably. Assuming that the spectral weight is concentrated at the point $\omega = a_t$, where a_t is a real function of t and setting $\rho_t(\omega) = 2\pi\delta(\omega - a_t)$ we arrive at the Loewner equation

$$\frac{dg_t(z)}{dt} = \frac{2}{g_t - a_t}. \quad (4.10)$$

The Loewner equation describes the growth of a curve or trace γ_t with endpoint z_t , $0 < t < \infty$, in the upper half complex z -plane. The time-dependent conformal transformation g_t maps the simply connected domain $\mathbf{H} \setminus \gamma_t$, i.e., the half plane excluding the curve γ_t back to the w half plane. At a given time instant t the tip of the curve z_t is determined by $g_t(z_t) = a_t$, i.e., the point where Eq. (4.10) develops a singularity. The topological properties and shape of the curve are encoded in the real function a_t which lives on the real axis in the w -plane. As a_t develops in time the tip of the curve z_t determined by $z_t = g_t^{-1}(a_t)$ traces out a curve. Since the domain $\mathbf{H} \setminus \gamma_t$ must be simply connected for the Riemann theorem to apply the curve or trace cannot cross itself or cross the real axis. Whenever the curve touches or intersect itself or the real axis the enclosed part will be excluded from the domain. In other, words, during the time progression the curve effectively absorbs part of the upper half plane. It is a deep property of Loewner evolution that the topological properties of a 2D non-crossing curve are entirely encoded by the real function a_t . The encoding works both ways: A given 2D non-crossing curve γ_t corresponds to a specific real function a_t , a given real function a_t yields a specific 2D non-crossing curve γ_t . A continuous a_t will yield a continuous curve γ_t . A discontinuous a_t in general gives rise to branching. Whether or not the curve intersects or touches itself is determined by the singularity structure of the drive a_t . In the case where the Hölder condition $\lim_{\tau \rightarrow 0} |(a_{t+\tau} - a_t)/\tau^{1/2}|$ is greater than 4 we have self-intersection. Note again that since the curve is defined indirectly by the singularity structure in Eq. (4.10) we cannot easily identify a curve parametrization and for example determine a tangent vector, etc. The mechanism underlying the Loewner equation is shown in Fig. 6.

C. Exact Solutions

In a series of simple cases one can solve the Loewner equation analytically [59,60]. For vanishing drive $a_t = 0$ we obtain the growing vertical stick discussed above. Correspondingly, a constant drive $a_t = a$ yields a vertical stick growing up from the point a on the real axis.

In the case of a linear drive $a_t = t$ the tip of the curve z_t is given by $z_t = 2 - 2\phi_t \cos \phi_t + 2i\phi_t$, where the phase ϕ_t is determined from the equations: $2 \ln r_t - r_t \cos \phi_t = 2 \ln 2 + t - 2$ and $r_t = 2\phi_t / \sin \phi_t$. By inspection $\phi_0 = 0$ and $\phi_\infty = \pi$. The curve thus approaches the asymptote $2\pi i$ for $t \rightarrow \infty$. For small t analysis yields $z_t \sim (2/3)t + 2i\sqrt{t}$, i.e., the trace approaches the origin with infinite slope. The square root drives $a_t = 2\sqrt{\kappa t}$ and $a_t = 2\sqrt{\kappa(1-t)}$, $0 < t < 1$ with a finite-time singularity can also be treated. In the first case, $a_t = 2\sqrt{\kappa t}$, the trace is a straight line $z_t = B \exp(i\phi) \sqrt{t}$ forming the angle ϕ with respect to the real axis. The amplitude B and phase ϕ depend on the parameter κ . The angle $\phi = (\pi/2)(1 - \kappa^{1/2}/(\kappa+4))^{1/2}$. For $\kappa = 0$, $\phi = \pi/2$ and we recover the perpendicular stick; for $\kappa \rightarrow \infty$, $\phi \rightarrow 0$ and the angle of intersection decreases to zero. In the second case, $a_t = 2\sqrt{\kappa(1-t)}$, the behavior of the trace is more complex. For $0 < \kappa < 4$ the trace forms a finite spiral in the upper half plane; for $\kappa = 4$ the trace has a glancing intersection with the real axis. For $4 < \kappa < \infty$ the trace hits the real axis in accordance with Hölder condition discussed above.

V. STOCHASTIC LOEWNER EVOLUTION

After these preliminaries we are in position to address stochastic Loewner evolution (SLE). The essential observation made by Oded Schramm [82] within the context of loop erased random walk was that the Markov and conformal properties of the measures or probability distributions for random curves generated by Loewner evolution imply that the random drive a_t must be proportional to an unbiased 1D Brownian motion.

A. Schramm's Theorem

The Loewner equation (4.10) generates a non-crossing curve in the upper half plane \mathbf{H} originating at the origin \mathbf{O} , given a continuous function a_t with initial value $a_0 = 0$. As a_t develops in time the tip of the curve z_t determined by the condition $g_t(z_t) = a_t$ traces out a curve or trace. In the case where a_t is a continuous random function the Loewner equation (4.10) likewise becomes a stochastic equation of motion yielding a stochastic map $g_t(z)$. As a result the trace determined by $g_t(z_t) = a_t$ or $z_t = g_t^{-1}(a_t)$ is a random curve. The issue is to establish a contact between the exploration processes defining interfaces in the lattice models, the scaling limit of these curves, and the curves generated by SLE. In the scaling limit we thus invoke the two properties discussed above: i) the Markov property in Eq. (2.12) and ii) the

conformal property in Eq. (3.1).

In order to demonstrate the surprising property that the Markov and conformal properties in combination imply that a_t must be a 1D Brownian motion we focus on chordal SLE which applies to a random curve or trace connecting two boundary points. Since the probability distribution or measure $P(\gamma)$ on the random curve γ using property ii) is assumed to be conformally invariant and since we by Riemann's theorem can map any simply connected domain to the upper half plane by means of a conformal transformation, we are free to consider curves in the upper half plane from the origin \mathbf{O} to ∞ parametrized with a time coordinate $0 < t < \infty$.

Imagine that we grow the curve from time $t = 0$ to time T driven by the function a_t , $0 < t < T$. The curve or trace is generated by the Loewner equation (4.10) with boundary condition $a_0 = 0$ and the trace z_t by $g_t(z_t) = a_t$ or $z_t = g_t^{-1}(a_t)$. With the chosen time parametrization we have $g_t(z) \sim z + 2t/z$ for $z \rightarrow \infty$ in the upper half plane. The map g_t thus uniformizes the trace, i.e., the tip z_t is mapped to a_t on the real axis in the w -plane. In order to invoke the Markov property we let the curve grow the time increment ΔT corresponding to the curve segment $\Delta\gamma$. The Markov property then implies that the distribution on $\Delta\gamma$ conditioned on the distribution on γ is the same as the distribution on $\Delta\gamma$ in the cut domain $\mathbf{H} \setminus \gamma$, i.e., the domain with the curve γ deleted; this stage is illustrated in Fig. 7.

Next, in order to implement the conformal property we shift the image by a_T in such a way that the curve segment $\Delta\gamma$ again starts at the origin \mathbf{O} . This is achieved by using the map $h_T = g_T - a_T$ which since $g_T(z_T) = a_T$ maps the tip z_T back to the origin; this construction is also depicted in Fig. 7. Moreover, the asymptotic behavior of h_T for large z is $h_T(z) \sim z - a_T - 2T/z$. Since the measure by assumption is unchanged under the conformal transformation h_T we infer that $\Delta\gamma$ growing the time ΔT from the origin has the same distribution as the segment $\Delta\gamma$ grown from time T to time $T + \Delta T$ conditioned on the segment γ grown up to time T . Moreover, since the segment γ from \mathbf{O} (AB) to C subject to the Markov property has become part of the boundary, as shown in Fig. 7, we also infer that the measure on $\Delta\gamma$ is independent of the measure on γ . Finally, applying $h_{\Delta T}$ we map the segment $\Delta\gamma$ to the origin as a common reference point as indicated in Fig. 7.

Since the random curves are determined by the random maps g_t and h_t driven by the random function a_t the issue is how to transfer the properties of the measure on the curve determined by the Markov and conformal properties to the measure on the random driving function a_t .

In order to combine the Markov properties arising from the analysis of the lattice models and the conformal invariance pertaining to critical random curves, we carry out the following steps. First we grow the curve γ from the origin \mathbf{O} to the tip z_T . Implying conformal invariance the curve is then uniformized back to the origin by means of h_T . The next step is to grow the curve segment $\Delta\gamma$ in time ΔT . This segment is subsequently absorbed by means of the map $h_{\Delta T}$. According to the Markov property the distribution of $\Delta\gamma$ from \mathbf{O} to $z_{\Delta T}$ is the same as the distribution of $\Delta\gamma$ grown from T to $T + \Delta T$ conditioned on γ grown from 0 to T . Since the curve γ is determined by the map h_t the distribution is reflected in h_t . In particular, the stochastic properties of the curve is transferred to the random function a_t generating the curve by the Loewner evolution. The last step is now to observe that absorbing

the segment $\Delta\gamma$ from \mathbf{O} to $z_{\Delta T}$ by means of $h_{\Delta T}$ is the same transformation as first applying the inverse map h_T^{-1} followed by the map $h_{T+\Delta T}$; in both cases the end result is the absorption of the initial curve $\gamma + \Delta\gamma$, see Fig. 7. As regards the measure or distribution we have the equivalence $h_{\Delta T}(z) \approx h_{T+\Delta T}(h_T^{-1}(z))$. Using the asymptotic form $h_t(z) \sim z - a_t - 2t/z$ we obtain $a_{T+\Delta T} - a_T \approx a_{\Delta T}$; note that \approx indicates identical distributions or measures.

In conclusion, the Markov property in combination with conformal invariance implies that $a_{T+\Delta T} - a_T$ is distributed like $a_{\Delta T}$ (stationarity) and that $a_{\Delta T}$ and $a_{\Delta T'}$ are independently distributed for non-overlapping time intervals ΔT and $\Delta T'$ (Markov property). Referring to Section III, A on Brownian motion as expressed in Eqs. (2.3) and (2.4), i.e., stationarity and independence, we infer that a_t is proportional to a Brownian motion of arbitrary strength κ , i.e., $a_t = \sqrt{\kappa}B_t$. Note that the reflection symmetry $x \rightarrow -x$ holding in the present context rules out a bias or drift in the 1D Brownian motion [6,13].

This is the basic conclusion reached by Schramm in the context of loop erased random walk. Driving Loewner evolution by means of 1D Brownian motion with different diffusion coefficient or strength κ we generate a one-parameter family of conformally invariant or scale invariant non-crossing random curves in the plane.

B. SLE Properties

Stochastic Loewner evolution is determined by the nonlinear stochastic equation of motion

$$\frac{dg_t}{dt} = \frac{2}{g_t - a_t}, \quad a_t = \sqrt{\kappa}B_t. \quad (5.1)$$

In the course of time a_t performs a 1D Brownian motion on the real axis starting at the origin $a_0 = 0$. a_t is a random continuous function of t and distributed according to $\sqrt{\kappa}B_t$. More precisely, a_t is given by the Gaussian distribution

$$P(a, t) = (2\pi t)^{-1/2} \exp[-a^2/2\kappa t], \quad (5.2)$$

with correlations

$$\langle (a_t - a_s)^2 \rangle = \kappa |t - s|. \quad (5.3)$$

First we notice that a constant shift of the drive a_t , $a_t \rightarrow a_t + b$, is readily absorbed by a corresponding shift of the map, $g_t \rightarrow g_t + b$. Moreover, using the scaling property of Brownian motion, $B_{\lambda^2 t} = \lambda B_t$, following from e.g. Eq. (2.5), we have $a_{\lambda^2 t} = \lambda a_t$ and we conclude from Eq. (5.1) that $g_t(z)$ has the same distribution as $(1/\lambda)g_{\lambda^2 t}(\lambda z)$, i.e., $g_{\gamma^2 t}(\gamma z) \approx \gamma g_t(z)$. Note that this dilation invariance is consistent since the origin $z = 0$ and $z = \infty$, the endpoints of curves, are preserved. Note also that the strength of the drive κ is an essential parameter which cannot be scaled away.

C. Curves - Hulls - Bessel Process

For vanishing drive, $\kappa = 0$, the SLE yields a non random vertical line from $z = 0$, i.e., the growing stick discussed in Sec. V.A. As we increase κ the curve becomes random with excursions to the right and to the left in the upper half plane. Up to a critical value of κ the random curve is simple; i.e., non-touching or non self-intersecting. At a critical value of κ the Brownian drive is so strong that the curve begins to intersect itself and the real axis. These intersection take place on all scales since the curve is self-similar or scale invariant. Denoting the curve by γ_t we observe that since Riemann's theorem uniformizing $\mathbf{H} \setminus \gamma_t$ to \mathbf{H} only applies to a simply connected domain, the regions enclosed by the self-intersections do not become uniformized but are effectively removed from \mathbf{H} . The curve γ_t together with the enclosed parts is called the hull \mathbf{K}_t and the mapping theorem applies to $\mathbf{H} \setminus \mathbf{K}_t$.

In order to analyze the critical value of κ we consider the stochastic equation for $h_t(z) = g_t(z) - a_t$. From Eq. (5.1) it follows that

$$\frac{dh_t}{dt} = \frac{2}{h_t} + \xi_t, \quad (5.4)$$

where $\xi_t = -da_t/dt$ is white noise with correlations $\langle \xi_t \xi_s \rangle = \kappa \delta(t - s)$.

The nonlinear complex Langevin equation (5.4) maps the tip of the curve z_t back to the origin. Likewise $\mathbf{H} \setminus \gamma_t$ is mapped onto \mathbf{H} . A point x on the real axis is mapped to $x_t = h_t(x)$ where x_t satisfies

$$\frac{dx_t}{dt} = \frac{2}{x_t} + \xi_t. \quad (5.5)$$

The Langevin equation (5.5) is known as the Bessel equation and governs the radial distance R from the origin of a Brownian particle in d dimensions.

Introducing $R = (\sum_{i=1}^d B_i^2)^{1/2}$ where B_i , $i = 1, \dots, d$, is a 1D Brownian motion with distribution $P(B, t) = (2\pi\kappa t)^{-1/2} \exp[-B^2/2\kappa t]$, we find $P(R, t) \propto (2\pi\kappa t)^{-d/2} R^{d-1} \exp[-R^2/2\kappa t]$ satisfying the Fokker-Planck equation $\partial P/\partial t = (\kappa/2)\partial^2 P/\partial R^2 - (\kappa(d-1)/2)\partial(P/R)/\partial R$, corresponding to the Langevin equation

$$\frac{dR}{dt} = \kappa \frac{d-1}{2R} + \xi_t. \quad (5.6)$$

For $d \leq 2$ Brownian motion is recurrent, i.e., the particle returns to the origin $R = 0$, for $d > 2$ the particle goes off to infinity. Setting $\kappa(d-1)/2 = 2$ we obtain $\kappa = 4/(d-1)$, i.e., $R \rightarrow \infty$ for $\kappa < 4$ and $R \rightarrow 0$ for $\kappa > 4$.

Since the tip of the curve z_t is mapped to a_t , i.e., $h(z_t) = 0$, the case $x_t \rightarrow \infty$ for $\kappa < 4$ corresponds to a curve never intersecting the real axis, i.e., the curve is simple. For $\kappa > 4$ we have $x_t \rightarrow 0$ corresponding to the case where the tip z_t intersects the real axis forming a hull. Since the curve is self-similar the intersections takes place on all scales and eventually the whole upper half plane is engulfed by the hull.

The marginal value $\kappa = 4$ can also be inferred from a simple heuristic argument [13]. For small κ we can ignore the noise in Eq. (5.5) and the particle is repelled

according to the solution $x_t^2 \sim 4t$. For large noise we ignore the nonlinear term and the noise can drive x_t to zero; we have $x_t^2 \sim \kappa t$. The balance is obtained for $\kappa = 4$.

In conclusion, for $\kappa \leq 4$ the curve is simple, for $\kappa > 4$ the curve intersects itself and the real axis infinitely many times on all scales, eventually the hull swallows the whole plane. For large κ the trace turns out to be plane-filling. The two cases $\kappa \leq 4$ and $\kappa > 4$ are depicted in Fig. 8.

D. Fractal Dimension

The SLE random curves are fractal. An important issue is thus the determination of the fractal dimension D in terms of the Brownian strength or SLE parameter κ . It has been shown that [45,46,79]

$$D = 1 + \frac{\kappa}{8} \quad \text{for } 0 \leq \kappa \leq 8, \quad (5.7)$$

for $\kappa \geq 8$ the fractal dimension locks onto 2 and the SLE curve is plane-filling.

In order to illustrate a typical SLE calculation we follow Cardy [13] in a heuristic derivation of Eq. (5.7). In order to evaluate D and in accordance with its definition [16,27] the standard procedure is to cover the object with disks of size ϵ and follow how the number of disks $N(\epsilon)$ of size ϵ scales with ϵ for small ϵ , i.e., $N(\epsilon) \propto \epsilon^{-D}$. However, since the SLE curve is random the argument has to be rephrased. Alternatively, we consider a disc of size ϵ located at a fixed position z and ask for the probability $P(z, \epsilon)$ that the SLE curve crosses the disk. The number of disks covering an area A is $N_A = A/\epsilon^2$, i.e., $P \propto \epsilon^{-D}/N_A$, and we infer $P(z, \epsilon) \propto \epsilon^{2-D}$, where D is the fractal dimension. Incorporating the Markov property we subject the curve to an infinitesimal conformal transformation, $h_{\delta t} = g_{\delta t} - a_{\delta t}$, transforming the point z to $w = g_{\delta t}(z) - a_{\delta t}$; moreover, all lengths are scaled by $|h'_{\delta t}(z)|$ [1]. Setting $z = x + iy$ and $w = x' + iy'$ we obtain expanding Eq. (5.4) $x' + iy' = 2\delta t/(x + iy) - \sqrt{\kappa}\delta B_t$ or $x' = x + 2x\delta t/(x^2 + y^2) - \sqrt{\kappa}\delta B_t$, $y' = y - 2y\delta t/(x^2 + y^2)$, $\epsilon' = (1 - |h_{\delta t}(z)|)\epsilon$, and $|h_{\delta t}| = 2(x^2 - y^2)/(x^2 + y^2)^2$. By conformal invariance the probability measure $P(x, y, \epsilon)$ is unchanged and we infer

$$P(x, y, \epsilon) = \langle P(x', y', \epsilon') \rangle_{\delta B}, \quad (5.8)$$

where we have averaged over the Brownian motion referring to the initial part of the curve which has been eliminated by the map $h_{\delta t}$. Expanding Eq. (5.8) to first order in δt and noting that $\langle (\delta B_t)^2 \rangle = \delta t$ we arrive at a partial differential equation for $P(x, y, \epsilon)$

$$\left(\frac{2x}{x^2 + y^2} \frac{\partial}{\partial x} - \frac{2y}{x^2 + y^2} \frac{\partial}{\partial y} + \frac{\kappa}{2} \frac{\partial^2}{\partial x^2} - \frac{2(x^2 - y^2)}{(x^2 + y^2)^2} \epsilon \frac{\partial}{\partial \epsilon} \right) P = 0. \quad (5.9)$$

Since $P(x, y, \epsilon) \propto \epsilon^{2-D}$ we have $\epsilon \partial P / \partial \epsilon = (2 - D)P$ and the determination of D is reduced to an eigenvalue problem. By inspection one finds

$$P \propto \epsilon^{1-\kappa/8} y^{(\kappa-8)^2/8\kappa} (x^2 + y^2)^{(\kappa-8)/2\kappa}, \quad (5.10)$$

and we identify the fractal dimension $D = 1 + \kappa/8$ for $\kappa < 8$; for $\kappa > 8$ another solution yields $D = 2$.

VI. RESULTS AND DISCUSSION

Stochastic Loewner evolution based on Eq. (5.1) generates conformally invariant non-crossing random curves in the upper half plane starting at the origin and going off to infinity. This is the case of chordal SLE, where the random curve connects two boundary points (the origin \mathbf{O} and infinity ∞). Another case is radial SLE for random curves connecting a boundary point and an interior point in a simply connected domain [6,13,21]. Radial SLE is governed by another stochastic equation and will not be discussed here.

A. Phase transitions - Locality - Restriction - Duality

1. Phase Transitions

SLE exhibits two phase transitions; for $\kappa = 4$ and $\kappa = 8$. For $0 < \kappa \leq 4$ the random curve is non-intersecting, i.e., a simple random continuous curve from \mathbf{O} to ∞ . For $4 < \kappa \leq 8$ the curve is self-intersecting on all scales. The curve together with the excluded regions form a hull which in the course of time absorbs the upper half plane. For κ just above 4 the half plane is eventually absorbed but the trace does not visit all regions, i.e., the hull is not dense. As we approach $\kappa = 8$ the trace becomes more dense and the hull becomes plane-filling. This is also reflected in the fractal dimension $D = 1 + \kappa/8$. For $\kappa > 8$ the hull is plane-filling, i.e., $D = 2$. As we increase the strength of the Brownian drive further the excursions of the trace to the right and left in the upper half plane become more pronounced and the hull becomes vertically compressed. These results have been obtained by Rohde and Schramm [79] and Lawler et al. [69]. The various phases of SLE are depicted in Fig. 8. In Fig. 9 we have depicted numerical renderings of SLE traces for various values of κ (with permission from V. Beffara, <http://www.umpa.ens-lyon.fr/~vbeffara/simu.php>).

2. Locality - Restriction

In addition to the phase transitions at $\kappa = 4$ and $\kappa = 8$, there are special values of κ where SLE shows a behavior characteristic of the scaling limit of specific lattice models: The locality property for $\kappa = 6$ and the restriction property for $\kappa = 8/3$. The issue here is the influence of the boundary on the SLE trace.

To illustrate the locality property, consider for example the SLE trace originating at the origin and purporting to describe the scaling limit of a domain wall in the lattice model. Due to the long range correlations at the critical point it is intuitively clear that a deformation of the boundary, e.g., a bulge \mathbf{L} on the real axis to the right of the origin, will influence the trace and push it to the left. A detailed analysis show that only for $\kappa = 6$ is the trace independent of a change of the boundary, i.e., the trace does not feel the boundary until it encounters a boundary point [71,75]. Returning to the lattice models the locality property for $\kappa = 6$ applies specifically

to the percolation case where the interface generated by the exploration process is governed by a local rule and the model has a geometric phase transition.

The restriction property is less obvious to visualize but basically states that the distribution of traces conditioned not to hit a bulge \mathbf{L} on the real axis away from the origin is the same as the distribution of traces in the domain where \mathbf{L} is part of the boundary, i.e., in the domain $\mathbf{H} \setminus \mathbf{L}$. Analysis shows that the restriction property only applies in the case for $\kappa = 8/3$. Among the lattice models only the scaling limit of self-avoiding random walk (SAW), where the measure is uniform, conforms to the restriction property and thus corresponds to $\kappa = 8/3$ [75].

3. Duality

For $\kappa > 4$ the SLE generates a hull of fractal dimension $D > 3/2$. The boundary, external perimeter, or frontier of the hull is again a simple conformally invariant random curve characterized by the fractal dimension \bar{D} . Using methods from 2D quantum gravity Duplantier [53] has proposed the relationship,

$$(D - 1)(\bar{D} - 1) = \frac{1}{4}, \quad (6.1)$$

between the fractal dimension of the hull and its frontier. This result has been proved by Beffara for $\kappa = 6$, i.e., the percolation case [46]. Inserting in Eq. (5.7) we obtain for the corresponding SLE parameter the duality relation

$$\kappa \bar{\kappa} = 16. \quad (6.2)$$

B. Loop Erased Random Walk (LERW)

Whereas the scaling limit of random walk, i.e., Brownian motion, does not fall in the SLE category because of self-crossings rendering Riemann's mapping theorem inapplicable, variations of Brownian motion are described by SLE.

Loop erased random walk (LERW) where loops are removed along the way is by construction self-avoiding and was introduced as a simple model of a self-avoiding random walk. LERW was studied by Schramm in his pioneering work [82]. LERW has the Markov property and has been proved to be conformally invariant in the scaling limit and described by SLE for $\kappa = 2$ [69]. According to Eq. (5.7) LERW has the fractal dimension $D = 5/4$. Also, since $\kappa < 4$ LERW is non-intersecting. A simulation of LERW based on SLE is shown in Fig. 9a.

C. Self-avoiding random walk (SAW)

Self-avoiding random walk (SAW) is a random walk conditioned not to cross itself. SAW has been used to model polymers in a dilute solution and has a uniform

probability measure. Since SAW satisfies the restriction property it is conjectured in the scaling limit to fall in the SLE class with $\kappa = 8/3$ [61,62,63,74], yielding the fractal dimension $D = 4/3$. We note that Flory's mean field theory [15] for the size R of a polymer composed of N links (monomers) scales like $R \sim N^\nu$, where $\nu = 3/(2+d)$ for $d \leq 4$. By a box covering we infer $N \sim R^D$ where D is the fractal dimension, i.e., $D = (2+d)/3$. In $d = 2$ we obtain $D = 4/3$ in accordance with the SLE result. SLE induced SAW in the scaling limit is shown in Fig. 9b.

D. Percolation

The scaling limit of site percolation was conjectured by Schramm [82] to fall in the SLE class for $\kappa = 6$. Subsequently, the scaling limit of site percolation on a triangular lattice has been proven by Smirnov [83,84]. Percolation exhibits a geometrical phase transition. In the exploration process defining a critical interface the rule for propagation is entirely local. The lack of stiffness as for example in the Ising case to be discussed below results in a strongly meandering path winding back and in the scaling limit intersecting earlier part of the path. Since $\kappa > 4$ the path together with the enclosed part, i.e., the hull, eliminates the whole plane in the course of time. As discussed above the locality property is specific to percolation and yields $\kappa = 6$. The fractal dimension of the percolation interface is according to Eq. (5.7) $D = 7/4$. We note that D is close to 2, i.e., the percolation interface nearly covers the plane densely. A series of new results and a proof of Cardy's conjectured formula for the crossing probability have appeared; we refer to [6,13,21] for details. Using the duality relation (6.2) the frontier of the percolation hull is a simple SLE curve for $\kappa = 8/3$, corresponding to SAW. In Fig. 9c we have depicted a SLE generated percolation interface.

E. Ising Model - O(n) Models

The Ising model in Eq. (2.6) is a special case of the O(n) model defined by the Hamiltonian

$$H = -J \sum_{\langle ij \rangle} \vec{\sigma}_i \vec{\sigma}_j, \quad (6.3)$$

where $\vec{\sigma}_i = (\sigma_1, \dots, \sigma_n)$ is an n-component unit vector associated with the site i . For $n = 1$ we recover the Ising model, $n = 2$ is the XY-model [14], and $n = 3$ the Heisenberg model.

By means of the Fortuin-Kasteleyn (FK) transformation based on a high temperature expansion the configurations of the O(n) model can be described by clusters or graphs on a dual lattice [55]. The crossing domain wall in Fig. 1 is thus a special case of a FK graph if we interpret the representation as a triangular Ising model. It has been conjectured that n is related to the SLE parameter κ by

$$n = -2 \cos(4\pi/\kappa) \quad \text{for } 8/3 \leq \kappa \leq 4. \quad (6.4)$$

In the Ising case $n = 1$ and we have $\kappa = 3$ yielding the fractal dimension $D = 11/8$ for the Ising domain wall [86]. Since $\kappa < 4$ the Ising domain wall is non-intersecting. Unlike the percolation case, the Ising interface is stiffer due to the interaction. We also note that the scaling limit of spin cluster boundaries in the Ising model recently has been proven to correspond to SLE for $\kappa = 3$ [85]. The interface is shown in Fig. 9d.

F. SLE - Conformal Field Theory

Whereas conformal field theory (CFT) is based on the concept of a local field $\phi(r)$ and its correlations and therefore only access the underlying geometry indirectly through field correlations, SLE directly produces conformally invariant geometrical objects. A major issue is therefore the connection between CFT and SLE [39,40,51]. In CFT the central charge c plays an important role in delimiting the universality classes of the variety of lattice models yielding conformal field theories in the scaling limit. Percolation thus corresponds to the central charge $c = 0$, whereas the Ising model is associated with the central charge $c = 1/2$. It has been conjectured that the connection between the SLE parameter κ and the central charge c is given by

$$c = \frac{(6 - \kappa)(3\kappa - 8)}{2\kappa} = 1 - 6\frac{(\kappa - 4)^2}{4\kappa}. \quad (6.5)$$

We note that $c < 1$ and, moreover, invariant under the duality transformation $\kappa \rightarrow 16/\kappa$.

G. SLE - 2D turbulence

There is an interesting application of SLE ideas in the context of 2D turbulence. The issue here is to analyze conformal invariance by comparing the statistical properties of geometrical shapes like domain walls with SLE traces with the view of determining the SLE parameter κ and the corresponding universality class.

In 3D turbulence is governed by the incompressible Navies-Stokes equation for the velocity field. Since the viscosity is only effective at small length scales 3D turbulence is characterized by a cascade of kinetic energy $(1/2)v^2$ from large scales (driving scale) to small scales (dissipation scale). In the inertial regime the energy spectrum $E(k)$ (k is the wavenumber) is characterized by the celebrated Kolmogorov 5/3 law [61], $E(k) \propto k^{-5/3}$, indicating an underlying scale invariance in turbulence.

In 2D the cascade picture is different. Since both kinetic energy and squared vorticity (enstrophy) are conserved in the absence of dissipation and forcing, two cascades coexist [67,68]. A direct cascade to small scales for the squared vorticity $\omega^2 = (\nabla \times v)^2$ with scaling exponent -3 and an inverse cascade to larger scales for the kinetic energy $(1/2)v^2$ with Kolmogoroff scaling exponent $-5/3$. The system is thus characterized by a fine scale vorticity structure together with a large scale velocity structure. Moreover, we can assume that the vorticity structure is equipartitioned, i.e, in equilibrium.

In order to investigate whether the scale invariance of the small scale vorticity structure can be extended to conformal invariance Bernard et al [48] have considered the statistics of the boundaries of vorticity clusters. By comparing the zero-vorticity isolines with SLE traces they find that cluster boundaries fall in the universality class corresponding to $\kappa = 6$, i.e., the case of percolation. Since 2D turbulence is a driven nonequilibrium system, this observation is very intriguing in particular since the correlations between vortices are long-ranged. A similar analysis [49] of the isolines in the inverse cascade in surface quasigeostrophic turbulence corresponds to $\kappa = 4$, i.e., from Eq. (6.4) the domain walls in the equilibrium XY model for $n = 2$. For comments on the application of SLE in turbulence we refer to Cardy [52].

H. SLE - 2D spin glass

It is a standing issue whether conformal field theory can be applied to disordered systems, in particular systems with quenched disorder. In recent work Amoroso et al. [38] and Bernard et al. [47] have considered zero temperature domain walls in the Ising spin glass [17]; see also [54]. The Ising spin glass is an equilibrium system with quenched disorder. The system is described by the Hamiltonian $H = -\sum_{\langle ij \rangle} J_{ij} \sigma_i \sigma_j$, where the random exchange constants J_{ij} are picked from a Gaussian distribution with zero mean. The glass transition is at $T = 0$ and the system has a two-fold degenerate ground state. Inducing a scale invariant domain wall between the two ground states and comparing with an SLE trace, it is found that both the Markov and conformal properties are obeyed and that the universality class corresponds to $\kappa \approx 2.3$.

I. Further remarks

In this discussion have left out several topics which have played an important role in the development and applications of SLE. We mention some of them below.

There is an interesting connection between LERW and the so-called uniform spanning tree (UST) [6,21,69,82]. A spanning tree is a collection of vertices and edges which form a tree, i.e., without loops or cycles. A uniform spanning tree is a random spanning tree picked among all possible spanning trees with equal probability. Consider the unique path between two vertices on a UST. Since the path lives on a tree it is by construction non-crossing and it turns out that it has the same distribution as LERW. The winding random curve enclosing the UST can be visualized as a random plane-filling Peano curve. In the scaling limit the Peano curve is described by SLE for $\kappa = 8$ with fractal dimension $D = 2$.

The q -state Potts model [37] constitutes a generalization of the Ising model; here the lattice variable takes q values. The model is defined by the Hamiltonian $H = -J \sum_{\langle ij \rangle} \delta_{\sigma_i \sigma_j}$, where $\sigma_i = 1, \dots, q$; the Ising model obtains for $q = 2$. Applying the high temperature FK representation the configurations can be represented by loops and domain walls. From considerations involving the fractal dimension [81] it has been conjectured that domain walls in the scaling limit of the Potts model fall in

the SLE category for $q = 2 + 2\cos(8\pi/\kappa)$, where $4 \leq \kappa \leq 8$. For $q = 2$ we recover the Ising case for $\kappa = 3$. In the limit $q \rightarrow 0$, the graph representation is equivalent to the uniform spanning tree described by SLE for $\kappa = 8$. For a numerical study of the three-state Potts model and its relation to SLE consult [56].

Standard SLE is driven by 1D Brownian motion producing a fractal curve. Ruskin et al. [80] have considered the case of adding a stable Lévy process with shape parameter α to the Brownian motion. Backing their analysis with numerics they find that the SLE trace branches and exhibit a 'phase transitions' related to self-intersections.

2D Brownian motion, the scaling limit of 2D random walk, is an incredibly complex fractal coil owing to the self-crossings on all scales. Although 2D Brownian motion because of self-crossing itself falls outside the SLE scheme, the outer frontier or perimeter of 2D random walk is a non-crossing and non-intersecting fractal curve which can be accessed by SLE. Verifying an earlier conjecture by Mandelbrot [27] it has been proven using SLE techniques [70] that the fractal dimension of the Brownian perimeter is $D = 4/3$, i.e, the same as the fractal dimension of self-avoiding random walk and the external perimeter of the percolation hull. Other characteristics of Brownian motion such as intersection exponents have also been obtained [71,72,73]; see also [77].

VII. FUTURE DIRECTIONS

Stochastic Loewner evolution represents a major step in our understanding of fractal shapes in the 2D continuum limit. By combining the Markov property (stationarity) with conformal invariance SLE provides a minimal scheme for the generation of a one-parameter family of fractal curves. The SLE scheme also provides calculational tools which have led to a host of new results. SLE is a developing field and we can on the mathematical front anticipate progress and proofs of some yet unproven scaling limits, e.g., the scaling limit of the FK representation of the Potts model and the scaling limit of SAW.

On the more physical front many issues also remain open. First there is the fundamental issue of the connection between the hugely successful but non-rigorous CFT and SLE. Here progress is already under way. In a series of papers Bauer and Bernard [39,40,41,42,43,44] have shown how SLE results can be derived using CFT methods. Cardy [51] have considered a multiple SLE process and the connection to Dyson's Brownian process and random matrix theory. The analysis of the CFT-SLE connection still remains to be analyzed further.

An obvious limitation of SLE is that it only addresses critical domain walls and not the full configuration of clusters and loops in for example the FK representation of the Potts model. In the case of critical percolation this problem has been addressed by Camia and Newman [50]. Another issue is how to provide SLE insight into spin correlations in the Potts or $O(n)$ models.

In the original formulation of SLE the Markov and conformal properties essentially requires a Brownian drive. It is clearly of interest to investigate the properties of

random curves generated by other random drives. Such a program has been initiated by Ruskin et al. [80] who considered adding a Lévy drive to the Brownian drive; see also work by Kennedy [64,65].

Since the SLE trace lives in the infinite upper half plane the whole issue of finite size effects remain open. In ordinary critical phenomena the concept of a Kadanoff block construction and the diverging correlation length near the transition lead to a theory of finite size scaling and corrections to scaling which can be accessed numerically. It is an open problem how to develop a similar scheme for SLE.

In statistical physics it is customary and natural to associate a free energy to a domain wall and an interaction energy associated with several domain walls. These free energy considerations are entirely absent in the SLE framework which is based on conformal transformations. A major issue is thus: Where is the free energy in all this and how do we reintroduce and make use of ordinary physical considerations and estimates [78].

VIII. BIBLIOGRAPHY

Books and Reviews

- [1] Ahlfors LV (1966) Complex analysis: an introduction to the theory of analytical functions of one complex variable. McGraw-Hill, New York
- [2] Ahlfors LV (1973) Conformal invariance: topics in geometric function theory. McGraw-Hill, New York
- [3] Ash RB, Doléans CA (2000) Probability & Measure Theory. Academic Press, San Diego
- [4] Bak P (1999) How Nature Works: The Science of Self-Organized Criticality. Springer, New York
- [5] Bauer M, Bernard D (2004) Loewner Chains. arXiv:cond-mat/0412372
- [6] Bauer M, Bernard D (2006) 2D growth processes: SLE and Loewner chains. Physics Reports, 432:115-221
- [7] Baxter RJ (1982) Exactly solved models in statistical mechanics. Academic Press, London
- [8] Binney JJ, Dowrick NJ, Fisher AJ, Newman MEJ (1992) The Theory of Critical Phenomena. Clarendon Press, Oxford
- [9] Cardy J (1987) Conformal invariance. In Phase Transitions and Critical Phenomena, vol 11, eds. Domb C and Lebowitz JL, Academic Press, London
- [10] Cardy J (1993) Conformal field theory comes of age. Physics World, June, 29-33
- [11] Cardy J (1996) Scaling and Renormalization in Statistical Physics. Cambridge University Press, Cambridge
- [12] Cardy J (2002) Conformal Invariance in Percolation, Self-Avoiding Walks and Related Problems. Plenary talk given at TH-2002, Paris; arXiv:cond-mat/0209638
- [13] Cardy J (2005) SLE for theoretical physicists. Ann. Phys. 318:81-118; arXiv:cond-mat/0503313
- [14] Chaikin PM, Lubensky TC (1995) Principles of Condensed Matter Physics. Cambridge University Press, Cambridge
- [15] de Gennes PG (1985) Scaling concepts in polymer physics, Cornell University Press, Ithaca
- [16] Feder J (1988) Fractals (Physics of Solids and Liquids). Springer, New York
- [17] Fischer KH, Hertz JA (1991) Spin Glasses. Cambridge University Press, Cambridge
- [18] Gardiner CW (1997) Handbook of Stochastic Methods. Springer-Verlag, New York

- [19] Gong S (1999) The Bieberbach Conjecture. R.I. American 19. Mathematical Society, International Press, Providence
- [20] Jensen HJ (2000) Self-Organized Criticality: Emergent Complex Behavior in Physical and Biological Systems. Cambridge University Press, Cambridge
- [21] Kager W, Nienhuis B (2004) A guide to Stochastic Loewner evolution and its application. J. Stat. Phys. 115:1149-1229
- [22] Kauffman SA (1996) At Home in the Universe: The Search for the Laws of Self-Organization and Complexity. Oxford University Press, Oxford
- [23] Landau LD, Lifshitz EM (1959) Theory of Elasticity. Pergamon Press, Oxford
- [24] Lawler GF (2005) Conformally invariant processes in the plane. Mathematical Surveys, 114, AMS, Providence, RI
- [25] Lawler GF (2004) ICTP Lecture Notes Series,
- [26] Ma S-K. (1976) Modern theory of critical phenomena. Frontiers in Physics, vol 46, Benjamin, Reading
- [27] Mandelbrot B (1987) The Fractal Geometry of Nature. W.H. Freeman & Company
- [28] Nicolis G (1989) Exploring Complexity: An Introduction. W.H. Freeman & Company
- [29] Nienhuis B (1987) Coulomb gas formulation of two-dimensional phase transitions. In Phase Transitions and Critical Phenomena, vol 11, eds. Domb C and Lebowitz JL, Academic Press, London
- [30] Pfeuty P, Toulouse G (1977) Introduction to the Renormalization Group and to Critical Phenomena. Wiley, New York
- [31] Reichl LE (1998) A Modern Course in Statistical Physics. Wiley, New York
- [32] Stanley HE (1987) Introduction to Phase Transitions and Critical Phenomena. Oxford University Press, Oxford
- [33] Stauffer D, Aharony A (1994) Introduction To Percolation Theory. CRC
- [34] Strogatz S (2003) Sync: The Emerging Science of Spontaneous Order. Hyperion
- [35] Werner W (2004) Random planar curves and Schramm-Loewner evolutions. Springer Lecture Notes in Mathematics 1840:107-195; arXiv: math.PR/0303354
- [36] Wilson KG, Kogut J (1974) The renormalization group and the ϵ expansion. Physics Reports, 12:75-199
- [37] Wu FY (1982) The Potts model. Rev. Mod. Phys. 54:235-268

Primary literature

- [38] Amoruso C, Hartmann AK, Hastings MB, Moore MA (2006) Conformal Invariance and Stochastic Loewner Evolution Processes in Two-Dimensional Ising Spin

- Glasses. Phys. Rev. Lett. 97:267202(4); arXiv:cond-mat/0601711
- [39] Bauer M, Bernard D (2002) SLE $_{\kappa}$ growth processes and conformal field theory. Phys. Lett. B 543:135-138; arXiv: math.PR/0206028
- [40] Bauer M, Bernard D (2003) Conformal field theories of Stochastic Loewner evolutions. Comm. Math. Phys. 239:493-521; arXiv: hep-th/0210015
- [41] Bauer M, Bernard D (2003) SLE martingales and the Viasoro algebra. Phys. Lett. B 557: 309-316; arXiv: hep-th/0301064
- [42] Bauer M, Bernard D (2004) Conformal transformations and the SLE partition function martingale. Annales Henri Poincare 5:289-326; arXiv:math-ph/0305061
- [43] Bauer M, Bernard D (2004) CFTs of SLEs: the radial case. Phys.Lett. B 583:324-330; arXiv:math-ph/0310032
- [44] Bauer M, Bernard D (2004) SLE, CFT and zig-zag probabilities. Proceedings of the conference ‘Conformal Invariance and Random Spatial Processes’, Edinburgh, July 2003; arXiv:math-ph/0401019
- [45] Beffara V (2002) The dimension of SLE curves; arXiv:math.PR/0211322
- [46] Beffara V (2003) Hausdorff dimensions for SLE $_6$. Ann. Probab. 32:2606-2629; arXiv:math.PR/0204208
- [47] Bernard D, Le Doussal P., Middleton AA (2006) Are Domain Walls in 2D Spin Glasses described by Stochastic Loewner Evolutions. arXiv:cond-mat/0611433
- [48] Bernard D, Boffetta G, Celani A, Falkovich G (2006) Conformal invariance in two-dimensional turbulence. Nature Physics, 2:124-128
- [49] Bernard D, Boffetta G, Celani A, Falkovich G (2007) Inverse Turbulent Cascades and Conformally Invariant Curves. Phys. Rev. Lett. 98:024501(4); arXiv: nlin.CD/0602017
- [50] Camia F, Newman CM (2003) Continuum nonsimple loops and 2D critical percolation. arXiv: math.PR/0308122
- [51] Cardy J (2003) Stochastic Loewner evolution and Dyson’s circular ensembles. J. Phys. A 36: L379-L408; arXiv: math-ph/0301039
- [52] Cardy J (2006) The power of two dimensions. Nature Physics, 2:67-68
- [53] Duplantier B (2000) Conformally Invariant Fractals and Potential Theory. Phys. Rev. Lett. 84:1363-1367; arXiv:cond-mat/9908314
- [54] Fisch R (2007) Comment on ”Conformal invariance and stochastic Loewner evolution processes in two-dimensional Ising spin glasses. arXiv:0705.0046
- [55] Fortuin CM, Kasteleyn PW (1972) On the random cluster model. Physica 57:536-564
- [56] Gamsa A, Cardy J (2007) SLE in the three-state Potts model - a numerical study; arXiv:0705.1510

- [57] Gruzberg IA, Kadanoff LP (2004) The Loewner Equation: Maps and Shapes. *J. Stat. Phys.* 114:1183-1198; arXiv:cond-mat/0309292
- [58] Kadanoff LP (1966) Scaling laws for Ising models near T_c . *Physics* 2:263-271
- [59] Kadanoff LP, Berkenbusch MK (2004) Trace for the Loewner equation with singular forcing. *Nonlinearity* 17:R41-R54; arXiv:cond-mat/0402142
- [60] Kager W, Nienhuis B, Kadanoff LP (2004) Exact Solutions for Loewner Evolutions. *J. Stat. Phys.* 115:805-822
- [61] Kennedy T (2002) Monte Carlo Tests of Stochastic Loewner Evolution Predictions for the 2D self-avoiding walk. *Phys. Rev. Lett.* 88:130601(4); arXiv:math.PR/0112246
- [62] Kennedy T (2004) Conformal invariance and Stochastic Loewner evolution predictions for the 2D Self-Avoiding walk - Monte Carlo tests. *J. Stat. Phys.* 114:51-78; arXiv: math.PR/0207231
- [63] Kennedy T (2005) Monte Carlo comparisons of the self-avoiding walk and SLE as parameterized curves. arXiv:math.PR/0510604v1
- [64] Kennedy T (2006) The length of an SLE - Monte Carlo studies. arXiv:math.PR/0612609v1
- [65] Kennedy T (2007) Computing the Loewner driving process of random curves in the half plane. arXiv:math.PR/0702071v1
- [66] Kolmogorov AN (1941) Dissipation of energy in the locally isotropic turbulence. *Dokl. Akad. Nauk SSSR* 30:9-13; reprinted in *Proc. R. Soc. Lond. A* 434:9-13 (1991)
- [67] Kraichnan RH (1967) Inertial ranges in two-dimensional turbulence. *Phys. Fluids.* 10:1417-1423
- [68] Kraichnan RH, Montgomery D (1980) Two-dimensional turbulence. *Rep. Prog. Phys.* 43:567-619
- [69] Lawler GF, Schramm O, Werner W (2001) Conformal invariance of planar loop-erased random walks and uniform spanning trees. *Ann. Prob.* 32:939-995; arXiv:math.PR/0112234
- [70] Lawler GF, Schramm O, Werner W (2001) The dimension of the planar Brownian frontier is $4/3$. *Math. Res. Lett.* 8:401-411; arXiv: math.PR/00010165
- [71] Lawler GF, Schramm O, Werner W (2001) Values of Brownian intersections exponents I: half plane exponents. *Acta Mathematica* 187:237-273; arXiv:math.PR/9911084
- [72] Lawler GF, Schramm O, Werner W (2001) Values of Brownian intersections exponents II: plane exponents. *Acta Mathematica* 187:275-308; arXiv:math.PR/0003156
- [73] Lawler GF, Schramm O, Werner W (2002) Values of Brownian intersections exponents III: two-sided exponents. *Ann. Inst. Henri Poincaré* 38:109-123; arXiv:

math.PR/0005294

[74] Lawler GF, Schramm O, Werner W (2002) On the scaling limit of planar self-avoiding walk. Fractal geometry and application, A jubilee of Benoit Mandelbrot, Part 2, 339-364, Proc. Sympos. Pure Math., 72, Part 2, Amer. Math. Soc., Providence, RI, 2004; arXiv: math.PR/0204277

[75] Lawler GF, Schramm O, Werner W (2003) Conformal restriction: The chordal case. J. Amer. Math. Soc. 16:917-955; arXiv: math.PR/0209343

[76] Löwner K (Loewner C) (1923) Untersuchungen über schlichte konforme Abbildungen des Einheitskreises. I. Math. Ann. 89:103-121

[77] Mackenzie D (2000) Taking the Measure of the Wildest Dance on Earth. Science 290:1883-1884

[78] Moore M (2007) private communication

[79] Rohde S, Schramm O (2001) Basic properties of SLE. Ann. Math., vol 161:879-920; arXiv: mathPR/0106036

[80] Rushkin I, Oikonomou P, Kadanoff LP, Gruzberg IA (2006) Stochastic Loewner evolution driven by Levy processes. J. Stat. Mech. (2006) P01001(21); arXiv:cond-mat/0509187

[81] Saleur H, Duplantier B (1987) Exact determination of the percolation hull exponent in two dimensions. Phys. Rev. Lett. 58:2325-2328

[82] Schramm O (2000) Scaling limit of loop-erased random walks and uniform spanning trees. Israel J. Math. 118:221-288; arXiv:math.PR/9904022

[83] Smirnov S (2001) Critical percolation in the plane: conformal invariance, Cardy's formula, scaling limits. C. R. Acad. Sci. Paris Ser. I Math, 333(3):239-244

[84] Smirnov S, Werner W (2001) Critical exponents for two-dimensional percolation. Math. Res. Lett. 8:729-744

[85] Smirnov S (2006) Towards conformal invariance of 2D lattice models. Proceedings of the International Congress of Mathematicians (Madrid, August 22-30, 2006), European Mathematical Society 2:1421-1451

[86] Vanderzande C, Stella AL (1989) Bulk, surface and hull fractal dimension of critical Ising clusters in $d = 2$. J. Phys. A: Math. Gen. 22:L445-L451

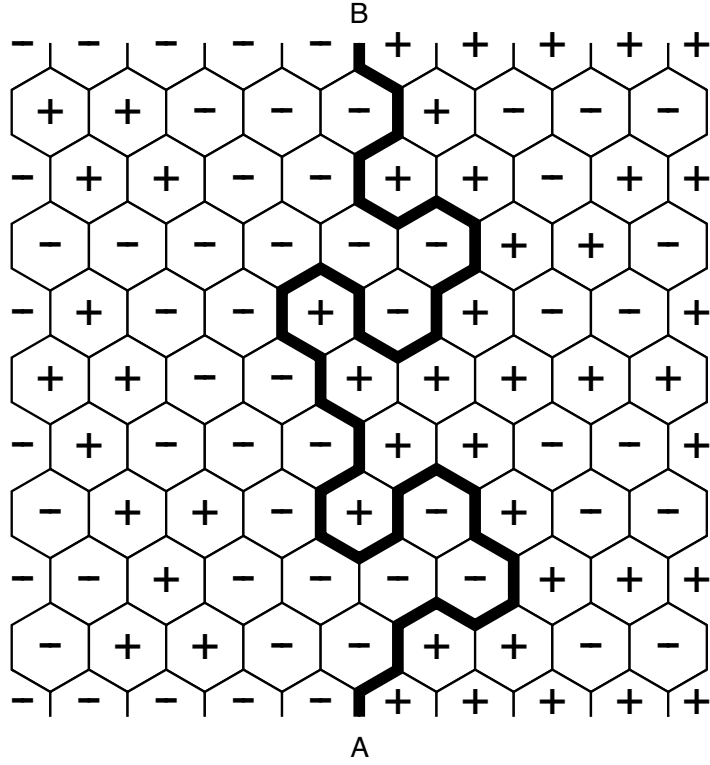


FIG. 1: We depict site percolation on a triangular lattice in the upper half plane at the percolation threshold. The critical concentration is $p_c = 1/2$. The occupied sites are denoted 'plus', the empty sites 'minus'. The boundary conditions enforce a meandering domain wall from A to B.

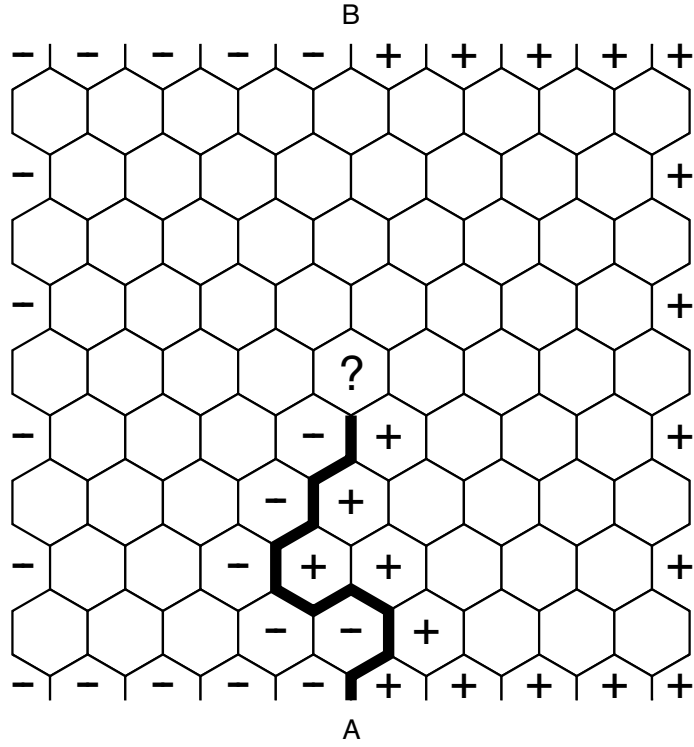


FIG. 2: We depict the growth process in the percolation case. The percolation threshold is at $p_c = 1/2$. The interface imposed by the boundary conditions originates at the boundary point A and progresses towards the boundary point B .

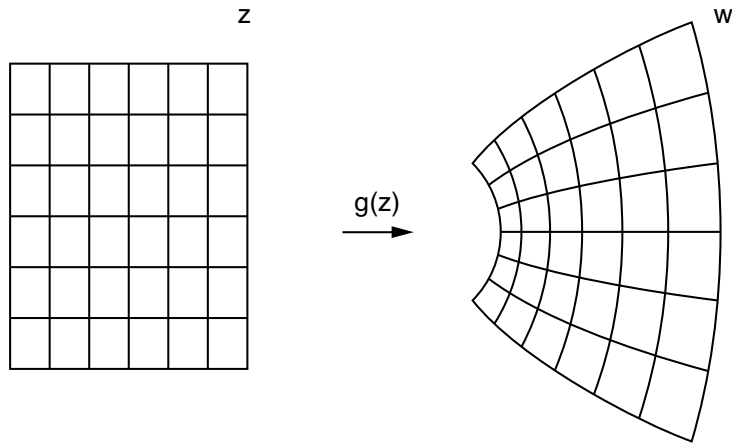


FIG. 3: We depict a conformal transformation from the complex z plane to the complex w plane. We note the angle-preserving property, i.e., a shear-free transformation. The map in the figure is given by $w = z^2$.

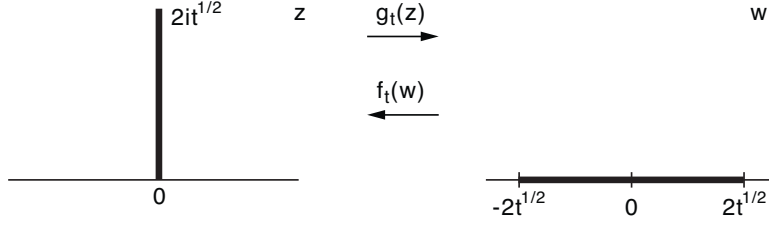


FIG. 4: We depict the growing stick corresponding to the conformal transformation $w = \sqrt{z^2 + 4t}$. The vertical cut in the z plane extends from the origin to the point $(0, 2it^{1/2})$. The right and left faces of the cut are mapped to the real axis from $-2t^{1/2}$ to $+2t^{1/2}$, the endpoint to the origin, in the complex w plane.

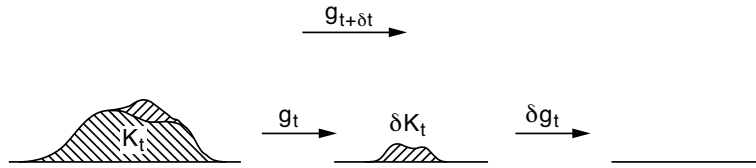


FIG. 5: The combination of maps involved in the derivation of the Loewner equation. First the map g_t eliminates the hull K_t . Subject to the growth in the time interval δt the incremental hull δK_t is subsequently absorbed by the infinitesimal map δg_t . Correspondingly, the hull $K_{t+\delta t}$ is absorbed by the map $g_{t+\delta t}$ in one step.

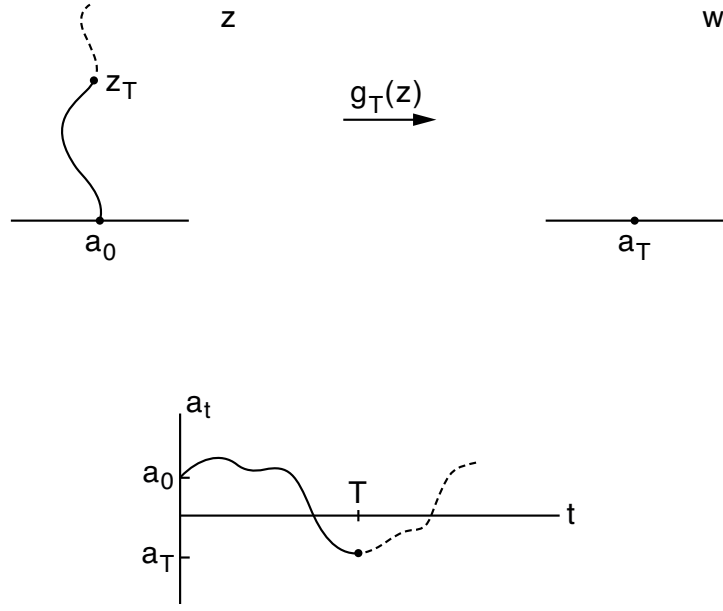


FIG. 6: The mechanism in the Loewner equation. The curve in the upper half complex z plane generated by the Loewner equation is mapped onto a finite but growing segment of the real axis of the complex w plane. The endpoint z_T is mapped to the real number a_T . As a_t develops in time and makes excursions along the real axis the endpoint z_t of the curve grows into the upper half plane.

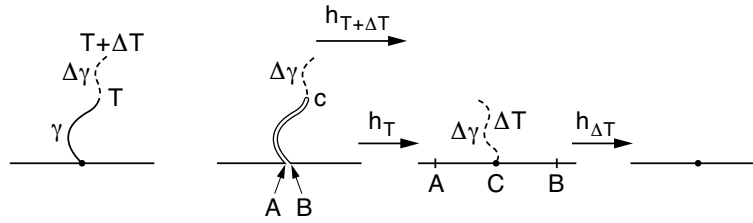


FIG. 7: The figure depicts the construction in the derivation of SLE. The first step implements the Markov property by turning the curve γ into a cut. Subsequently, the conformal transformation h_T maps γ back to the origin. Finally, the map $h_{\Delta T}$ maps the segment $\Delta\gamma$ to the origin. The complete process is also implemented by $h_{T+\Delta T}$. The combination of the Markov property and conformal invariance implies that a_t performs a Brownian motion

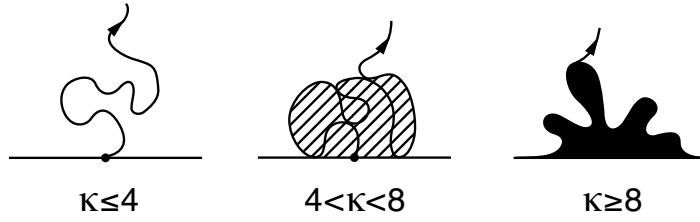


FIG. 8: The figures depict the phases of SLE. For $\kappa \leq 4$ the SLE trace is a simple non-intersecting scale invariant random curve from the origin to infinity with a fractal dimension between 1 and $3/2$. For $4 < \kappa \leq 8$ the SLE curve is self-intersecting on all scales and also intersects the real axis on all scales. The curve together with the enclosed regions, the hull, eventually exhausts the upper half plane. The scale invariant hull has a fractal dimension ranging between $3/2$ and 2. For $\kappa \geq 8$ the fractal dimension of the hull locks onto 2 and the scale invariant hull is dense and plane-filling.

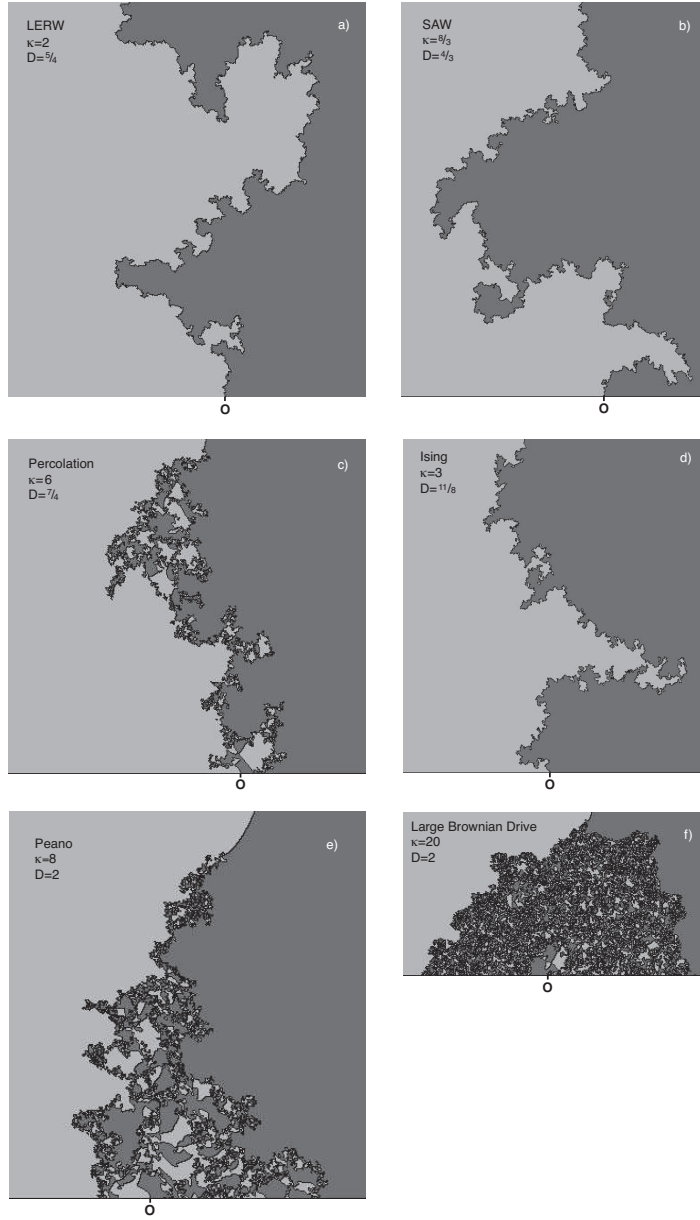


FIG. 9: We depict a numerical renderings of SLE for a variety of κ values. In a) we show loop erased random walk (LERW) for $\kappa = 2$ with fractal dimension $D = 5/4$. In b) we illustrate the case of self-avoiding random walk (SAW) for $\kappa = 8/3$ and fractal dimension $D = 4/3$; both LERW and SAW have $\kappa > 4$ and are simple scale invariant random curves. In c) we depict site percolation for $\kappa = 6$ with fractal dimension $D = 7/4$. Since $\kappa > 4$ the percolation case is self-intersecting and duality implies that the boundary or frontier of the hull is described by a SLE curve for $\kappa = 16/6 = 8/3$, i.e., the case of SAW. In d) we show the Ising case for $\kappa = 3$ and fractal dimension $D = 11/8$. In e) we depict the limiting case $\kappa = 8$ and fractal dimension $D = 2$. The hull is dense and plane-filling. The frontier of the hull corresponds to the SLE case $\kappa = 16/8 = 2$, i.e., the case of LERW. The so-called uniform spanning tree (UST) has the same properties as LERW and the SLE case for $\kappa = 8$ can thus be thought of as a random plane filling Peano curve wrapping around the UST. Finally, in f) we show the SLE trace and hull for $\kappa = 20$ and $D = 2$. Because of the large Brownian excursions the plane-filling hull is vertically compressed (with permission from V. Beffara: <http://www.umpa.ens-lyon.fr/~vbeffara/simu.php>).